Design of a short electro-optic modulator based on SiGe HBT structure

Shengling Deng, Tuhin Guha Neogi, Joseph Novak, John McDonald, Z. Rena Huang

Department of Electrical, Computer, and System Engineering, Rensselaer Polytechnic Institute, 110 8th Street, Troy, NY 12180, USA

Abstract: A SiGe electro-optic modulator operating at wavelength of 1.55μm is proposed. The "ON" state voltage is set at 1.4V. The arm of the MZI waveguide required to generate a π phase shift is 73.6μm, and the total attenuation loss is 3.95dB. The rise and fall delay time is 70.9ps and 24.5ps, respectively.

OCIS codes: (130.4110) Modulator; (130.3120) Integrated optics devices; (230.2090) Electro-optic devices;

References and links

1. A. Liu, L. Liao, D. Rubin, H. Nguyen, B. Ciftcioglu, Y. Chetrit, N. Izhaky, and M. Paniccia, "High-speed optical modulation based on carrier depletion in a silicon waveguide," Opt. Express **15**(2), 660–668 (2007).
2. F. Y. Gardes, G. T. Reed, A. P. Knights, and G. Mashanovich, "Evolution of optical modulation using majority carrier plasma dispersion effect in SOI", Proc. of SPIE 6898, 68980C–68980C–10 (2008).
3. A. Liu, R. Jones, L. Liao, D. Samara-Rubio, D. Rubin, O. Cohen, R. Nicolaescu, and M. Paniccia, "A high-speed silicon optical modulator based on a metal-oxide-semiconductor capacitor," Nature **427**(6975), 615–618 (2004).
4. Q. Xu, B. Schmidt, S. Pradhan, and M. Lipson, "Micrometre-scale silicon electro-optic modulator," Nature **435**(7040), 325–327 (2005).
5. Q. Xu, S. Manipatruni, B. Schmidt, J. Shakya, and M. Lipson, "12.5 Gbit/s carrier-injection-based silicon micro-ring silicon modulators," Opt. Express **15**(2), 430–436 (2007).
6. W. M. J. Green, M. J. Rooks, L. Sekaric, and Y. A. Vlasov, "Ultra-compact, low RF power, 10 Gb/s silicon Mach-Zehnder modulator," Opt. Express **15**(25), 17106–17113 (2007).
7. S. Deng, Z. R. Huang, and J. F. McDonald, "Design of high efficiency multi-GHz SiGe HBT electro-optic modulator," Opt. Express **17**(16), 13425–13428 (2009).
8. A. Liu, "Announcing the world's first 40G silicon laser modulator", http://blogs.intel.com/research/2007/07/40g_modulator.php.
9. J.-S. Rieh, D. Greenberg, A. Stricker, and G. Freeman, "Scaling of SiGe heterojunction bipolar transistors," Proc. IEEE **93**(9 Issue 9), 1522–1538 (2005).
10. J.-S. Rieh, M. Khater, G. Freeman, and D. Ahlgren, "SiGe HBT without selectively implanted collector (SIC) exhibiting f_{max}=310GHz and BV_{CEO}=2V," IEEE Trans. Electron. Dev. **53**, 2407–2409 (2006).
11. J. D. Cressler, and G. Niu, *Silicon-Germanium Heterojunction Bipolar Transistors* (Artech House, Inc, 2007).
12. R. A. Soref, and B. R. Bennett, "Kramers-Kronig analysis of electro-optical switching in silicon," SPIE Integr. Opt. Circuit Eng. **704**, 32–37 (1986).
13. R. D. Lareau, L. Friedman, and R. A. Soref, "Waveguided electro-optical intensity modulation in a Si/Ge_xSi_{1-x}/Si heterojunction bipolar transistor," Electron. Lett. **26**(20), 1653–1655 (1990).
14. A. Cutolo, M. Iodice, P. Spirito, and L. Zeni, "Silicon electro-optic modulator based on a three terminal device integrated in a low-loss single-mode SOI waveguide," J. Lightwave Technol. **15**(3), 505–518 (1997).

1. Introduction

The silicon-based electro-optic (EO) modulator is an indispensable building block for integrated lightwave circuits. The desired properties of an EO modulator include small footprint, fast switching speed, and low power consumption. For applications such as wavelength-division multiplexing (WMD), a device with broad spectrum width is also critical. The existence of many trade-offs in the underlining device physics makes it challenging to design a silicon EO modulator with overall high performance. For example, high modulation speed can be obtained from majority carrier depletion mechanism [1,2] or Metal-Oxide-Semiconductor (MOS) capacitor [3], but the device lengths are in the millimeter range. It has shown that incorporating resonant structures in an EO modulator can greatly boost up the speed and modulation efficiency [4,5], but it comes at the expense of reduced spectrum

#120157 - $15.00 USD Received 18 Nov 2009; revised 13 Jan 2010; accepted 14 Jan 2010; published 19 Jan 2010

bandwidth. Additionally, the resonant structures are usually sensitive to temperature fluctuation and susceptible to fabrication imperfections [6].

In this paper, we present the design and analysis of an EO modulator whose electrical structure is an NPN Heterojunction Bipolar Transistor (HBT) with a submicron emitter. Our previous paper reported a SiGe HBT EO modulator design with a rib waveguide width (i.e. the emitter lateral width) greater than 1μm [7], which exhibited a high modulation efficiency of L_π = 74μm in Mach-Zehender Interferometer (MZI) configuration, and an estimated bandwidth of 2.4GHz. The goal of this work is to design a new device that offers much enhanced performance in all device aspects compared to our previous design. In this new design, some additional electronic structures are included to make the device more practical, such as the shallow trenches made of SiO_2, the selected implanted collector (SIC) region, and the raised extrinsic base. The small cross-section of the device leads to enhanced EO interaction, enabling a reduced "ON" state voltage, i.e. 1.4V in the new design. The issue of doping profile and attenuation loss is also evaluated in this paper. At λ = 1.55μm with TM polarization, the EO modulator demonstrates a multiple gigahertz bandwidth with a device length of 73.6μm. To our knowledge, the proposed device provides the best combined bandwidth-length product compared to existing Si-based EO modulators reported up to date without employing optical resonator structures or complex travelling-wave electrodes [1,8].

2. Device structure design

2.1 Device schematic

A schematic of the cross-section of the proposed new HBT EO modulator is shown in Fig. 1, in which the geometric parameters are labeled. Details of the design and optimization of the parameters are to be presented in the next two subsections. A continuous monochromatic lightwave with wavelength chosen at λ = 1.55μm, is coupled into the EO modulator from the *x-y* plane, and propagates in the waveguide along the *z*-axis.

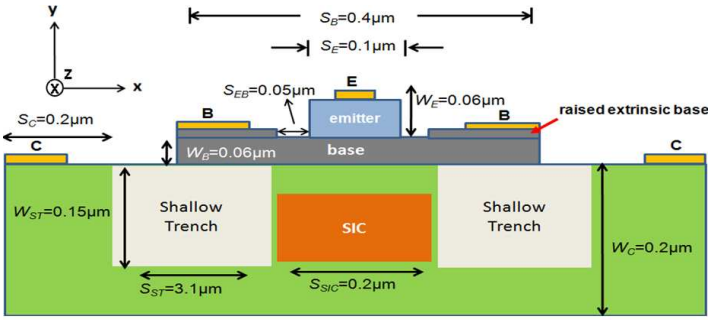

Fig. 1. Schematic of our HBT device cross-section

2.2 Design of device parameters

Both vertical and lateral scaling rules have been explored in pursuing ever increasing cutoff frequency (f_T) and the maximum oscillation frequency (f_{max}) in analog and RF circuits. The HBT in the EO modulator is used in switching mode, and requires large signal swing to maximize the carrier plasma modulation effect. Therefore, the speed of the HBT EO modulator is determined by its transient response, instead of f_T or f_{max}. However, it is shown that a well designed HBT following the scaling rules for f_{max} exhibits good digital switching response [9,10] as well. In this work, the guideline of the device design is to keep the critical parameters as close as possible to the state-of-the-art HBTs for maximized compatibility with SiGe foundry, and then to introduce necessary changes wherever required by the optical properties of the device.

Vertical scaling of the HBTs is often given higher priority than lateral scaling. Base thickness is the most important and the representative scaling parameter in the device design.

#120157 - $15.00 USD Received 18 Nov 2009; revised 13 Jan 2010; accepted 14 Jan 2010; published 19 Jan 2010

A thinner base reduces minority carrier transit time and enhances built-in electric field. Modern HBTs usually have an extremely thin base [11]. In this design, the base thickness (W_B) is chosen to be 60nm by considering the trade-off between the speed and the carrier plasma volume. The Ge composition in the base varies from 0 at the emitter-base (EB) junction to 20% at the base-collector (BC) junction. Another aspect in vertical scaling involves the SIC region, which was introduced to postpone the onset of Kirk effect, and also to maintain a satisfactory breakdown voltage BV_{CEO}. We keep the SIC region in our design, and set the total collector thickness to be 0.2μm, smaller than typical HBT devices. The choice of thinner collector in the design is to achieve better optical field confinement in the base region where the largest carrier density variation takes place. The lateral scaling of HBT reduces the emitter width (S_E). In our design, we choose $S_E = 0.1\mu m$.

The geometric parameters, shallow trench depth (W_{ST}) and width (S_{ST}), are key to the optical properties, and are optimized by combining qualitative analysis with a series of numerical simulations. Generally, a deeper trench confines lateral mode extension, thus favoring higher EO interaction. However, it leads to increased collector resistance, causing increased switch delay. Therefore, the trench should be deep enough for the satisfactory mode confinement, but should not cause severe speed degradation. A trench depth of $W_{ST} = 0.15\mu m$ is chosen for this design. The trench width S_{ST} has a more profound effect on the optical mode guiding, and is to be discussed in detail in section 2.4.

2.3 Doping profile design

As ultra-thin base thickness W_B is chosen, a non-negligible base resistance R_B is anticipated. In addition, the thin base makes the device more prone to base punch-through. A routine to combat these challenges is to elevate the base doping. For today's HBTs, the base doping is commonly above $10^{19}cm^{-3}$ [11]. In our design, however, the high doping is purposely avoided due to the concern of propagation loss. According to the empirical relations given in [12], the absorption coefficient is proportional to the doping, and as a result, the propagation loss increases exponentially. The estimated loss in a general waveguide increases sharply from 2.6×10^{-4}dB/μm to 2.6×10^{-2}dB/μm, when acceptor concentration increases from $10^{17}cm^{-3}$ to $10^{19}cm^{-3}$. For the same donor concentration change, the loss increases from 3.7×10^{-4}dB/μm to 3.7×10^{-2}dB/μm. The calculation is comparable with Soref's prediction [13]. Since the design objective is a modulator no longer than 100μm with a single digit dB loss, a doping level of $10^{18}cm^{-3}$ is chosen for the base region, and $10^{19}cm^{-3}$ for the emitter. The reduced doping in the base and the emitter will slow down the transient response, as one of the trade-offs.

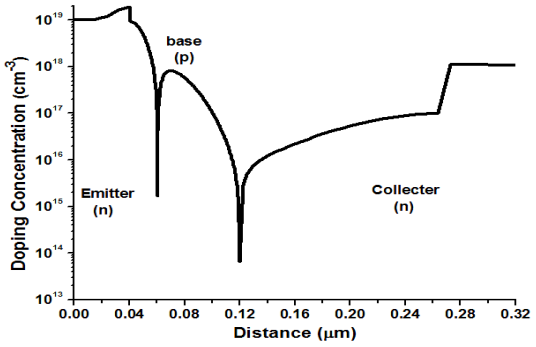

Fig. 2. Y-axis doping profile through the device center

Under thermal equilibrium condition, the estimated space charge region width in the base is 34.4nm on EB side and 3.2nm on BC side calculated by step junction approximation. The total depletion width of 37.6nm is much smaller than $W_B = 60nm$, suggesting that base punch-through is not a concern here. The 1D doping profile at the center of the device is shown in

#120157 - $15.00 USD Received 18 Nov 2009; revised 13 Jan 2010; accepted 14 Jan 2010; published 19 Jan 2010

Fig. 2. To reduce the collector series resistance, the reach-through regions under the collector contacts and the channels below the trenches are doped high.

2.4 Mode confinement consideration

Comparing to our earlier design, two shallow trenches, used to separate the base from the collector are explicitly added into this analysis. The shallow trenches also provide lateral confinement to the traveling light within the center of the device. The reach-through regions beneath the collector contacts construct two independent side-waveguides that are separated from the center by the shallow trenches. As the trench width is on the order of micrometer, there is a possibility of light coupling between the center-waveguide to the side-waveguides. The optical coupling is rather negative to the device performance since it not only causes reduced modulation efficiency, but leads to increased power loss since the side-waveguides are very lossy. To minimize the coupling, the shallow trench has to be sufficiently wide. However, an oversized trench is undesirable as it leads to longer current path, and thus higher series resistance in the collector. To find an optimal trench width, we tailored S_{ST} while monitoring the light propagation in the device. The simulation results show strong coupling when $S_{ST} \leq 1\mu m$. The coupling length, defined as the distance required to transfer the peak intensity from one waveguide to another, is about 60μm for $S_{ST} = 1\mu m$, more than 250μm for $S_{ST} = 2\mu m$. For $S_{ST} > 3\mu m$, no coupling is observed up to 300μm.

3. Device performance characterization

The device analysis includes the electrical and the optical aspects. The electrical properties are analyzed using a 2-D device simulation package MEDICI. The Philips unified model and the velocity saturation model are combined for mobility modeling, as is suggested by [11]. To account the excess carrier recombination and the heavy doping effects, the bandgap narrowing (BGN) model, the concentration dependent SRH (Shockley-Read-Hall) model, and the Auger recombination model are included. The optical properties of the waveguide are characterized with RSoft BeamProp, a simulation tool based on the Beam Propagation Method (BPM). The conversion from carrier density to 2-D refractive index map is accomplished by using the widely accepted empirical equations [12]. By importing the refractive index data into the BeamProp model, the phase delay and the propagation loss are calculated.

3.1 Plasma density change

To illustrate the plasma density change versus bias voltage, a 1-D carrier distribution along the *y*-axis is shown in Fig. 3. At the EB junction, significant carrier injection occurs when V_{BE} rises to above 0.8V. At a bias of $V_{BE} = 1.0V$, the electron density in the base exceeds the base doping level. As required by the charge neutrality, the hole density also increases greatly in the base. Contrary to most HBT devices in high frequency circuits, as has discussed earlier, the designed EO modulator is relatively lightly doped in the emitter. As a result, the hole injection from the base to the emitter is not negligible at high V_{BE}, despite of the heterojunction. From Fig. 3(b), we can see the hole density on the emitter side of the EB junction is comparable to that on the base side, when V_{BE} is above 1.0V. The emitter, the base, and the collector boundary can be found in Fig. 2. The hole injection into the emitter degrades the amplification factor β, a major small signal parameter defined as the ratio between the collector and the base current. The reason of β degradation is because that smaller fraction of the emitter current is carried by electron, the primary component that eventually contributes to the collector current. However, since the nature of the EO modulator is to utilize the storage carriers to regulate the effective indices of the MZI waveguide, the amplification factor β is not of our major concern. The hole injection into the emitter does bring a speed-efficiency tradeoff to the modulator operation: it slows down the device due to hole diffusion in the emitter; whereas the extra free carrier plasma is in favor of phase modulation efficiency.

At the BC junction, once V_{BE} surpasses $V_{CE} = 0.4V$, the junction becomes forward biased. In this condition, minority carriers also inject into both sides of the BC junction. The injection starts to be significant as the BC junction is turned on, as can be seen from the curves at V_{BE}

#120157 - $15.00 USD Received 18 Nov 2009; revised 13 Jan 2010; accepted 14 Jan 2010; published 19 Jan 2010

≥1.2V in Fig. 3. The strong minority carrier injection at the BC junction contributes to the free carrier plasma density in the base, and also extends the modulation region into the collector. As the deep saturation condition is chosen for the "ON" state, the speed suffers as a result.

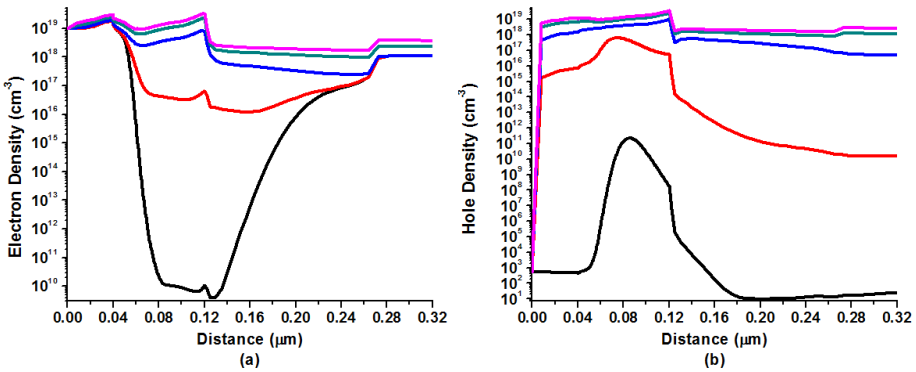

Fig. 3. (a) Electron density (b) Hole density along y-axis at the device center for V_{BE} = 0V, 0.8V, 1.0V, 1.2V, and 1.4V (from bottom to top in each plot)

3.2 Mode issues

The designed EO modulator is built on Si-on-insulator (SOI) wafers with a SiO_2 overglass as the top cladding. The SOI wafer is required due to the necessity of mode confinement in the vertical direction. Since the base contains most of the injected carriers, the optical field should have as large overlap with the base as possible. This demands that the collector to be very thin. Otherwise, the mode field will stretch deeply downwards, causing reduced field-plasma interaction with the base. With the above defined conditions, the core area of the waveguide is laterally confined by the shallow trenches and is vertically confined by the SiO_2 overglass on the top and the buffered oxide layer at the bottom.

The profile of the major electric fields E_y of the fundamental TM-like mode is plotted in Fig. 4 with a plot window smaller than the actual size of the computation window for clarity. The reach-through areas are not shown in this figure. It is indicated by the mode solver that the waveguide supports only fundamental TM-like mode. The electric field primarily sits in the collector with relatively weaker intensity in the base. Because of the small dimension and strong index contrast, significant amount of energy is guided in the SiO_2 layers. In summary, the plasma-induced index change provides an off-center perturbation in the waveguide core, which is not the most desired scenario. However, as limited by the HBT geometry, it is rather difficult to shift the peak of the field completely to the base region. At different bias voltages, the BPM simulation shows little change in mode profiles, which is starkly different from our previous design in which severe mode stretching was observed. The invariance of the mode contour is mainly attributed to the tight mode confinement provided by the closely placed shallow trenches in the lateral direction. The nearly fixed mode profile at high voltage greatly improves the modulation efficiency compared to our previous design.

#120157 - $15.00 USD Received 18 Nov 2009; revised 13 Jan 2010; accepted 14 Jan 2010; published 19 Jan 2010

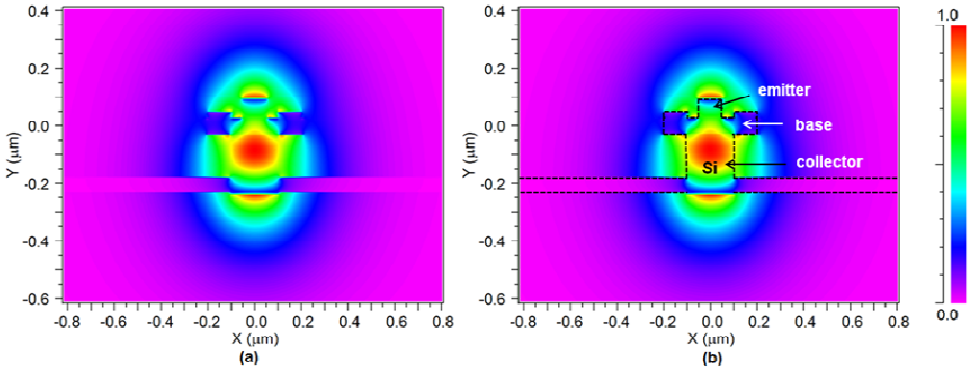

Fig. 4. (a) Major electric field E_y of TM-like mode at λ = 1.55μm (b) Mode overlap with the waveguide.

As a relatively complex structure, a possible polarization mixing problem is worth of further scrutiny since it could cause extinction ratio penalty of the MZI. A 3D FDTD computation is performed in a straight waveguide of nearly identical structure except that the raised extrinsic base regions are left out for simplicity. The absorption loss due to free carrier plasmas is also assumed zero in the FDTD simulation. The simulation computed the distribution and evolvement of all the six electromagnetic field components, that is, E_x, E_y, E_z, H_x, H_y, H_z.

The FDTD computation reveals that the E_y field, i.e. the major electric field of the TM-like mode is nearly the same as that calculated by using semi-vector BPM. Moreover, the amplitude and profile of the E_y do not vary as the wave propagates along the waveguide. Thus, it is confirmed that the proposed device structure only supports the fundamental mode for TM polarization wave. During the propagation, the TM-like mode does not convert into other modes either due to mode orthogonality. The amplitude of E_x, i.e. the major electric field of the TE-like wave exhibits position-dependent variation, suggesting multimode beats in the structure. If we limit the coupling to only TM-like polarized light in the HBT waveguide, theoretically there is no polarization conversion to TE along a straight waveguide so that polarization purity can be maintained. However, any curvature or fabrication imperfection of the HBT waveguide will inevitably induces a portion of the TM wave converting to TE wave. We will study the polarization mixing of curved HBT waveguide in the future.

3.3 Transient response

The transient response of the device is shown in Fig. 5. The collector-emitter is biased at V_{CE} = 0.4V. A rectangular voltage pulse applied at BE junction swings between V_{BE} = −1.4V (“OFF”) and 1.4V (“ON”) with 1ps ramp time. The “OFF” state is set at a negative voltage to reduce the minority carrier storage time during the switch-off process. The on and the off delay read from the plot, defined as 10%-90% of the steady-state current, is 70.9ps and 24.5ps, respectively. A current spike occurs at the very beginning stage of the turn-on or the turn-off process. We attribute it to the junction displacement current and the non-zero dV/dt when voltage ramps up or down. The spikes are lowered with prolonged ramp time, which validates our explanation.

#120157 - $15.00 USD Received 18 Nov 2009; revised 13 Jan 2010; accepted 14 Jan 2010; published 19 Jan 2010

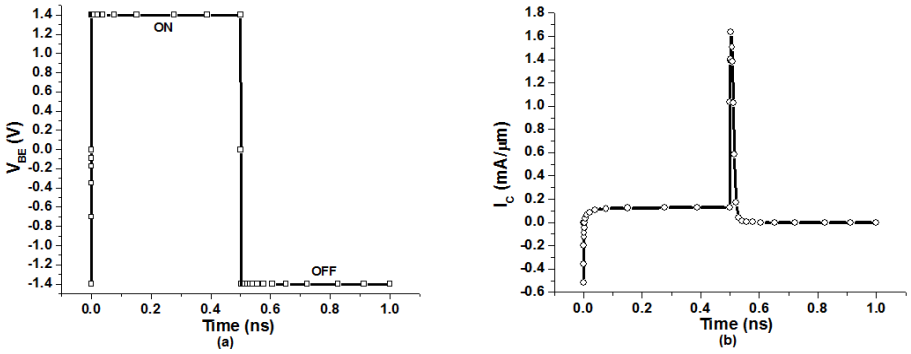

Fig. 5. Transient analysis: (a) input pulse V_{BE}, and (b) I_C response.

It is worth noting that the "ON" state voltage set for this switching is much higher than that for the HBT in logic circuits. Therefore, the transient response obtained here, although much faster than most carrier injection EO modulators, is no match with its counterpart in the logic circuit. Compared to the PIN EO modulator, the thin base combined with the built-in electric field in the HBT make a significant difference in speed. Additionally, the existence of the collector as a third terminal further reduces the response time in both the carrier built-up and the carrier removal process. As a three-terminal device, the HBT also allows easy manipulation of the speed and efficiency trade-off by adjusting the collector bias.

3.5 Device length, FoM, propagation loss, and power consumption

With biasing condition fixed, the most important parameter for characterizing modulator efficiency is the active waveguide length to introduce a phase delay by π. We denote the parameter as L_π. At V_{BE} = 1.4V, L_π is 73.6μm for the TM polarization, and is 80.2μm for the TE polarization. The corresponding voltage-length production, or the figure of merit (FoM), is 0.010V-cm and 0.011V-cm, for TM and TE respectively. The FoM value is better than our previous design as a result of the reduced bias.

Calculated from the imaginary part of the effective index, the unit attenuation for TM mode is 0.0228dB/μm for the "OFF" state, and 0.0536dB/μm for the "ON" state. The "OFF" state loss originates from the background doping, while the additional loss at the "ON" state is from the injected free carriers. Considering the device of L_π = 73.6μm, the "ON" state total loss is 3.95dB. Even though the loss per unit length in the HBT modulator is higher than its PIN counterpart, the total loss is comparable with many injection-type EO modulators [6,14].

The dynamic power of the device of 73.6μm length is evaluated as follows:

$$P_d = 0.5 \times f_S \times \int_0^{T_S} \left(i_C(t) V_{CE}(t) + i_B(t) V_{BE}(t) \right) dt \qquad (1)$$

where f_S is the switching frequency, and T_S is the pulse duration. The factor 0.5 in Eq. (1) accounts for the fact that the "ON" state appears with 50% possibility in a long random Non-Return-to-Zero (NRZ) pulse train. The minimum pulse width, or the maximum data rate, is limited by the response time. According to our transient analysis, the smallest T_S is 95.4ps, and the inverse of *Ts* gives a maximum Baud rate of 10.5Gbps. Admittedly, due to the unequal rise and fall time, the transmission of pulses with duration of 95.4ps is subject to certain extinction ratio penalty. Based on the above assumption, the estimated dynamic power is 288mW, equivalent to 27.4pJ/bit, which is higher than other carrier injection-type devices [6]. However, the proposed HBT can work much faster than most injection-type EO modulators. The high power consumption of the HBT EO modulator is mainly due to the high base current i_B, a result of severely degraded amplification factor β (β <1 at steady-state). A few parameters can be tailored to achieve smaller i_B, and thus lowering the power. For example, heavy emitter doping and thin base are both in favor of β, but leading to increased

#120157 - $15.00 USD Received 18 Nov 2009; revised 13 Jan 2010; accepted 14 Jan 2010; published 19 Jan 2010

waveguide propagation loss and reduced modulation efficiency. The modulation efficiency can be also traded for lower power by reducing V_{BE} or increasing V_{CE}.

4. Summary

In this paper, we proposed a new design of fast Si-based EO modulator using HBT structure. Compared to our earlier design, this new device exhibits well improved performance and has a much smaller footprint. The device is designed to be biased at V_{CE} = 0.4V and switched at base-emitter terminals with V_{BE} = ± 1.4V. A total turn-on and turn-off delay of 95.4ps is obtained in this condition. The dynamic power consumption is 27.4pJ/bit at the maximum transmission rate. For λ = 1.55μm of TM polarization, an interaction length of L_π = 73.6μm is required. The total attenuation loss of the L_π waveguide is 3.95dB. The exclusion of high Q resonators but adoption of a standard MZI configuration in the design make the proposed device more practical for deployment in wideband applications.

Acknowledgements

This work was in part supported by RPI internal fund, and in part by NSF (ECCS award # 0824068).

#120157 - $15.00 USD Received 18 Nov 2009; revised 13 Jan 2010; accepted 14 Jan 2010; published 19 Jan 2010